Electronic Supplementary Information:

Observation of Crystalline Change of Titanium Dioxide During Lithium Insertion by Visible Spectrum Analysis

Inho Nam,‡[a] Jongseok Park,‡[a] Soomin Park,[a] Seongjun Bae,[a] Young Geun Yoo,[a] Jeong Woo Han[b] and Jongheop Yi*[a]

[a.] School of Chemical and Biological Engineering, WCU Program of C_2E_2, ICP, Seoul National University, Seoul 08826, Republic of Korea. E-mail: jyi@snu.ac.kr

[b.] Department of Chemical Engineering, University of Seoul, Seoul 02504, Republic of Korea

Electronic Supplementary Information (ESI) available: Supplementary Fig.s S1-S10.

‡ These authors contributed equally to this work.

Supplementary Fig. S1-S10

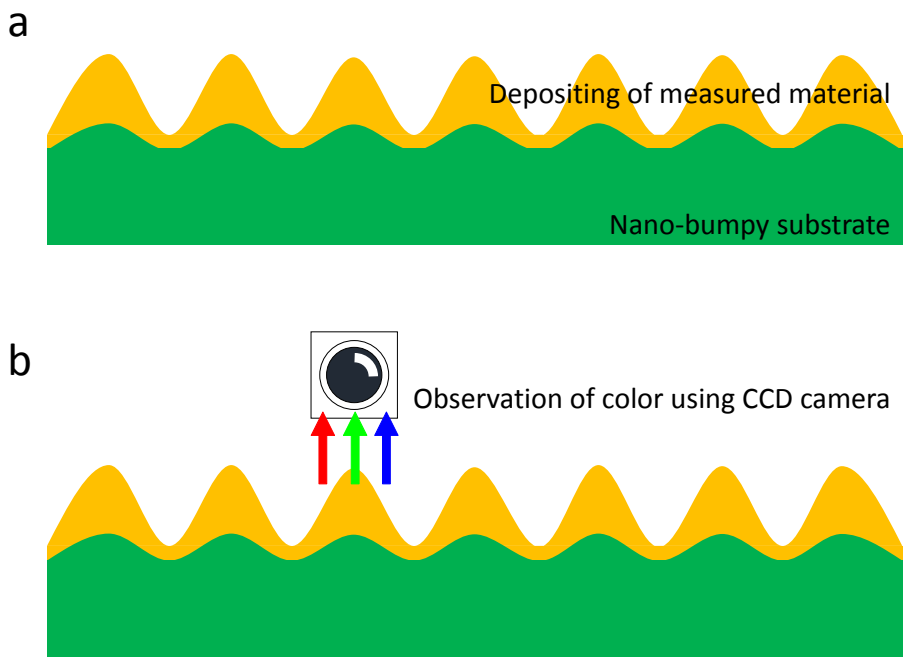

Supplementary Fig. S1. Schematic illustration of real-time observation with a charge-coupled device (CCD) camera. (a) A material to be measured (yellow) would be deposited forming a periodic nanostructure on a nano-bumpy substrate (green). (b) A structural color would appear by the wave interference on the nanostructure, which gives information on the change in the crystal structure.

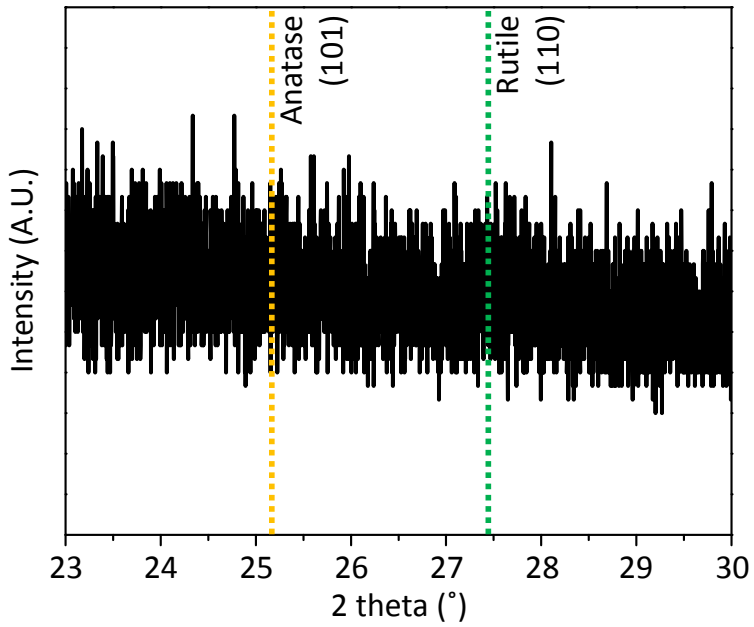

Supplementary Fig. S2. An XRD pattern of mixed-phase TiO_2 polymorph after lithium insertion reaction. Main peaks (anatase (101): 25.176°, rutile (110): 27.355°) disappear after complete lithium storage, confirming the variation in crystal structure during the reaction.

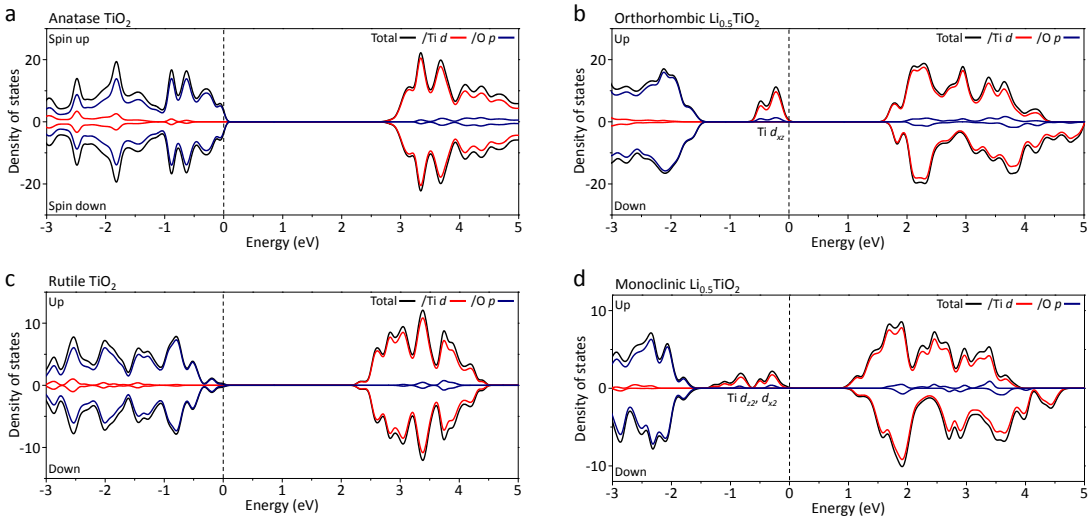

Supplementary Fig. S3. Ab-initio calculation of the density of states for each crystal involved in the system. Titanium d-band and oxygen p-band states are marked red and blue, respectively. The corresponding sum of the density of states is marked black. Electronic spin states are also involved as the signs (plus or minus) indicate. All the valence band edges were adjusted to 0 eV. (a) Density of states of anatase TiO_2. (b) the Resultant density of states of orthorhombic $Li_{0.5}TiO_2$ after Li insertion. Anatase TiO_2 goes through a dramatic reduction in energy band-gap (from ~3eV to ~1.8eV) due to the incorporation of the Ti d_{xz} state in the initially forbidden region by the lithium insertion to the crystal structure. (c) Density of states of rutile TiO_2. (d) Resultant density of states of monoclinic $Li_{0.5}TiO_2$ after Li insertion. A similar phenomenon of anatase occurs in the case of rutile TiO_2 (reduction in energy band-gap from ~2.2eV to ~1eV). In this case, Ti d_{z^2}, d_{x^2} levels are incorporated into the forbidden regions of rutile as the reaction with lithium proceeds.

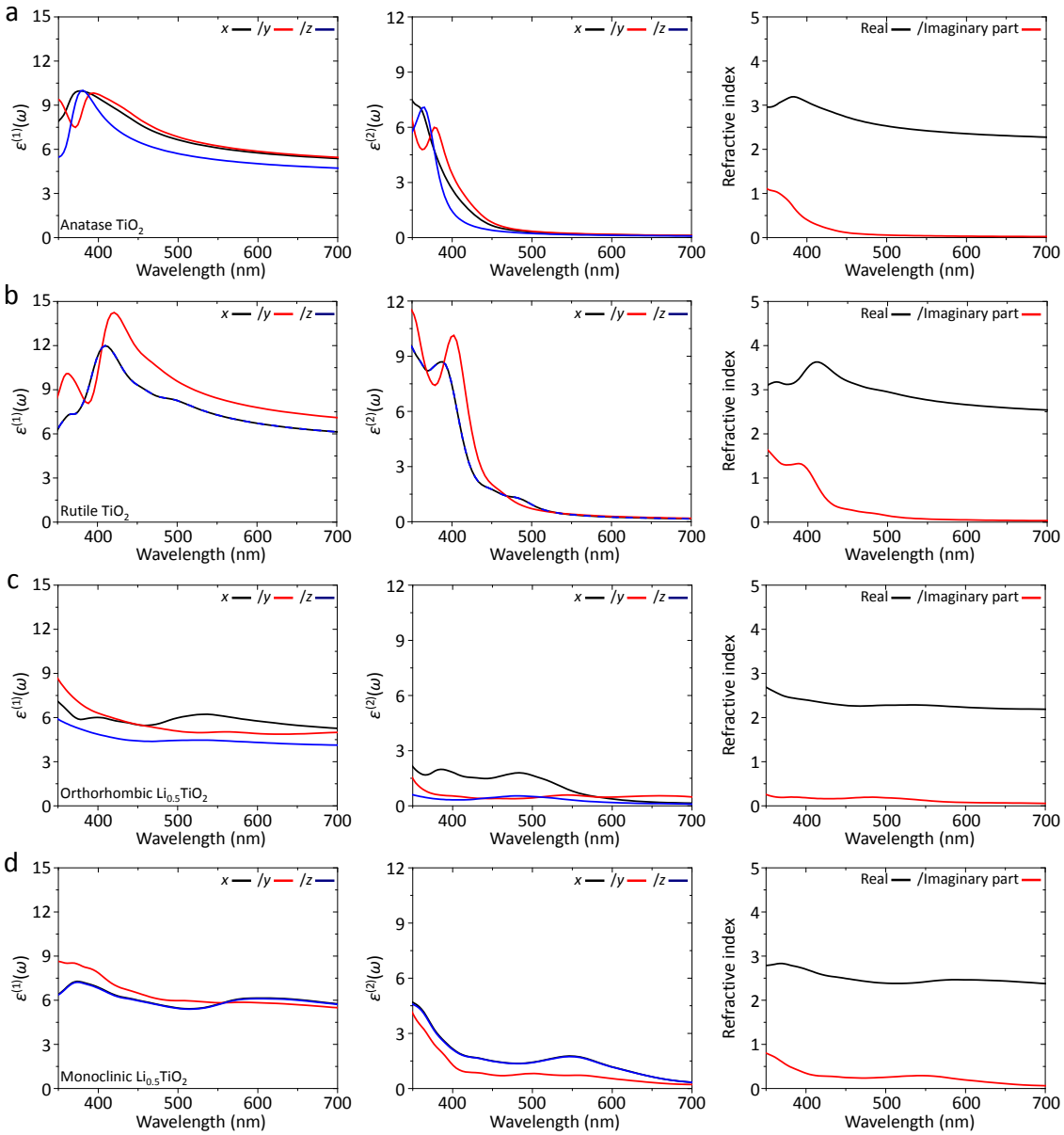

Supplementary Fig. S4. Calculated dielectric functions of wavelengths. (a,b,c, and d) Anatase, rutile TiO_2, orthorhombic, and monoclinic $Li_{0.5}TiO_2$, respectively. From left to right, real part and imaginary part of the dielectric function and resultant refractive indices are shown in order. Dielectric constants are functions of wavelengths and they are different for each axis (x, y and z) in the cartesian coordinate.

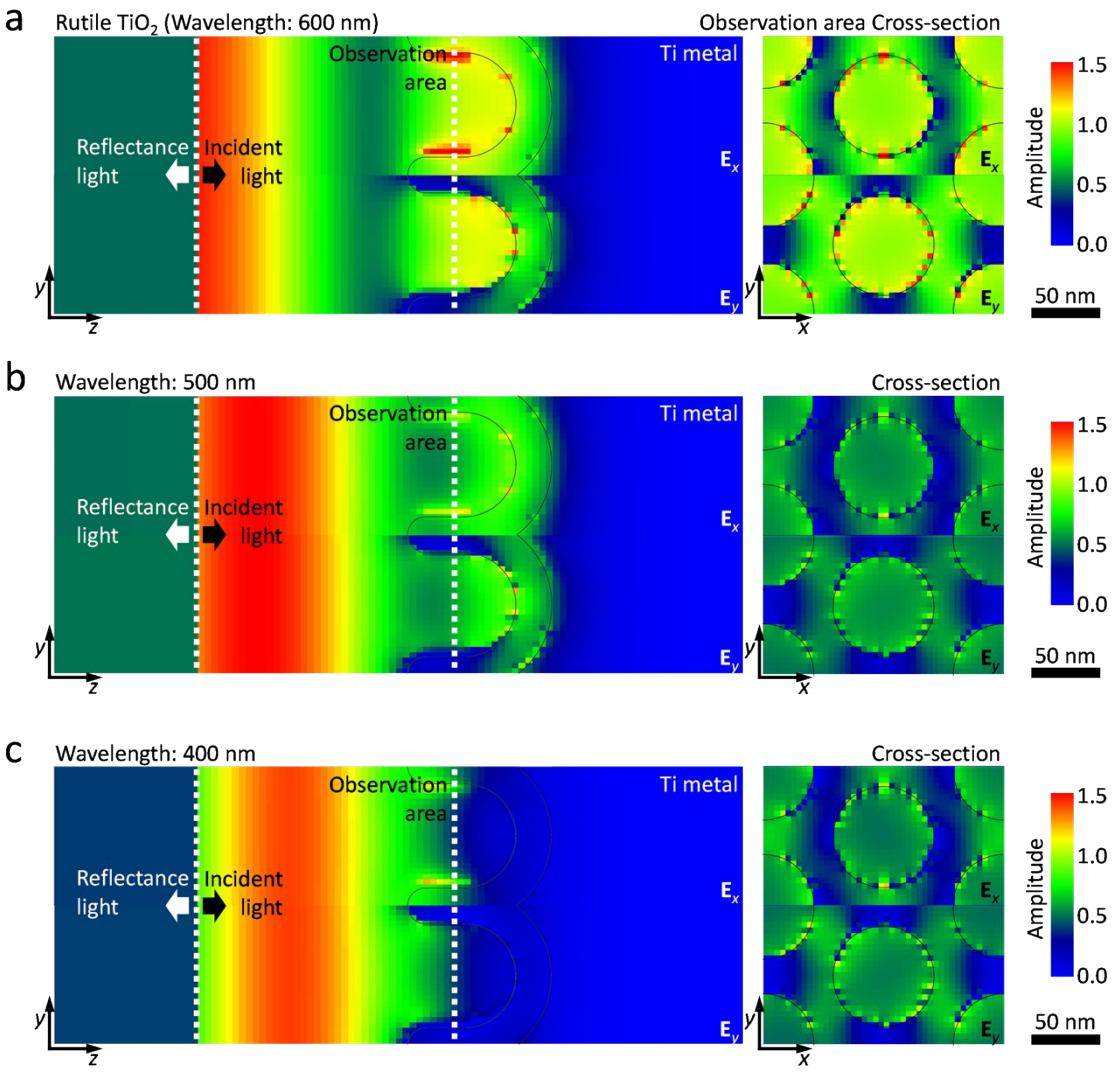

Supplementary Fig. S5. Simulated distribution of electric fields formed by the surface of rutile TiO_2 in the hexagonal nanostructure. Distribution of electric fields is demonstrated by contour mapping with a color gradient with corresponding amplitudes assigned on the right end of the bars. Representative electric fields are shown at (a) 600, (b) 500 and (c) 400 nm wavelength, respectively.

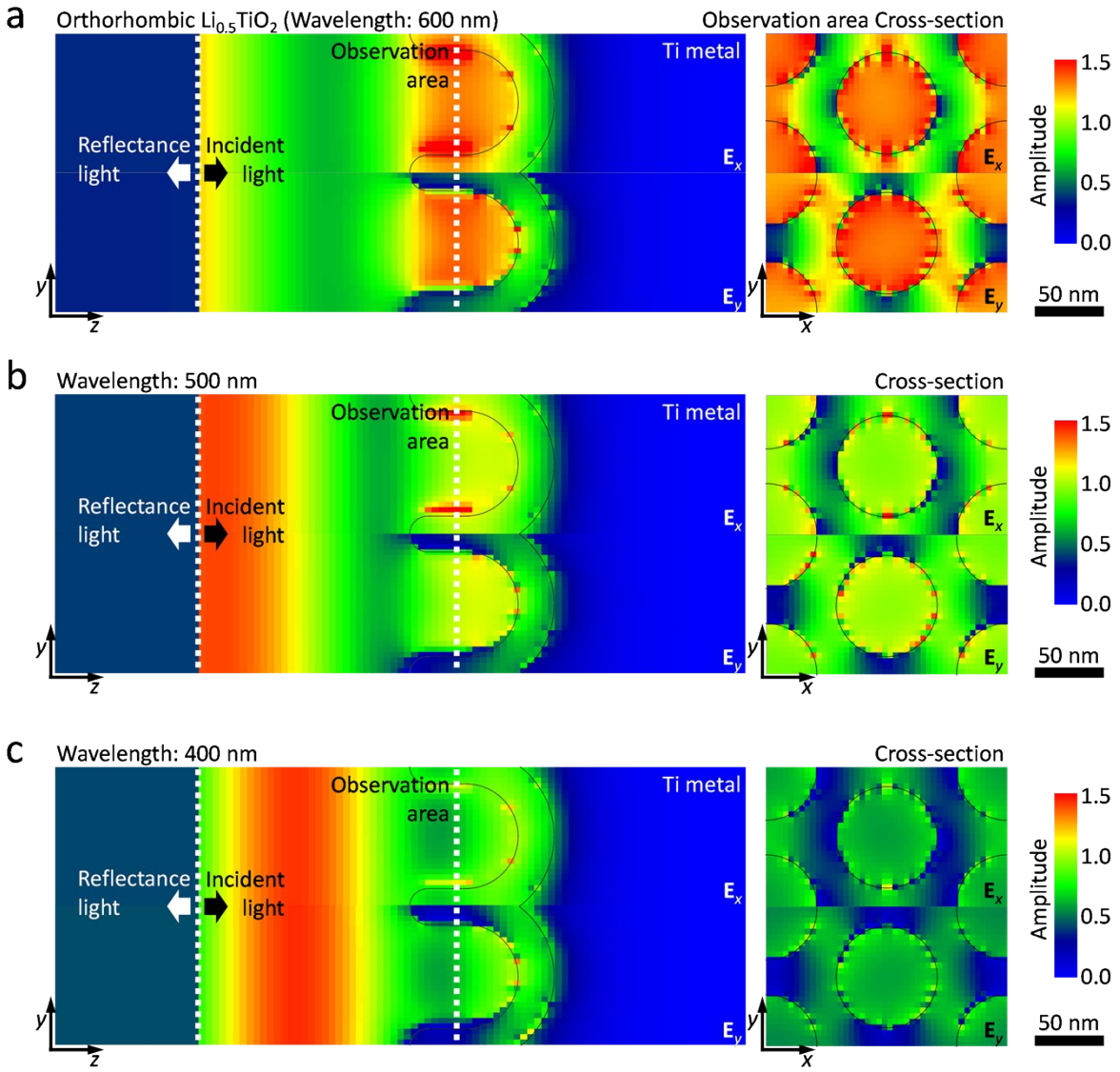

Supplementary Fig. S6. Simulated distribution of electric fields by the surface of orthorhombic $Li_{0.5}TiO_2$ in the hexagonal nanostructure. Representative electric fields are shown at (a) 600, (b) 500 and (c) 400 nm wavelength, respectively.

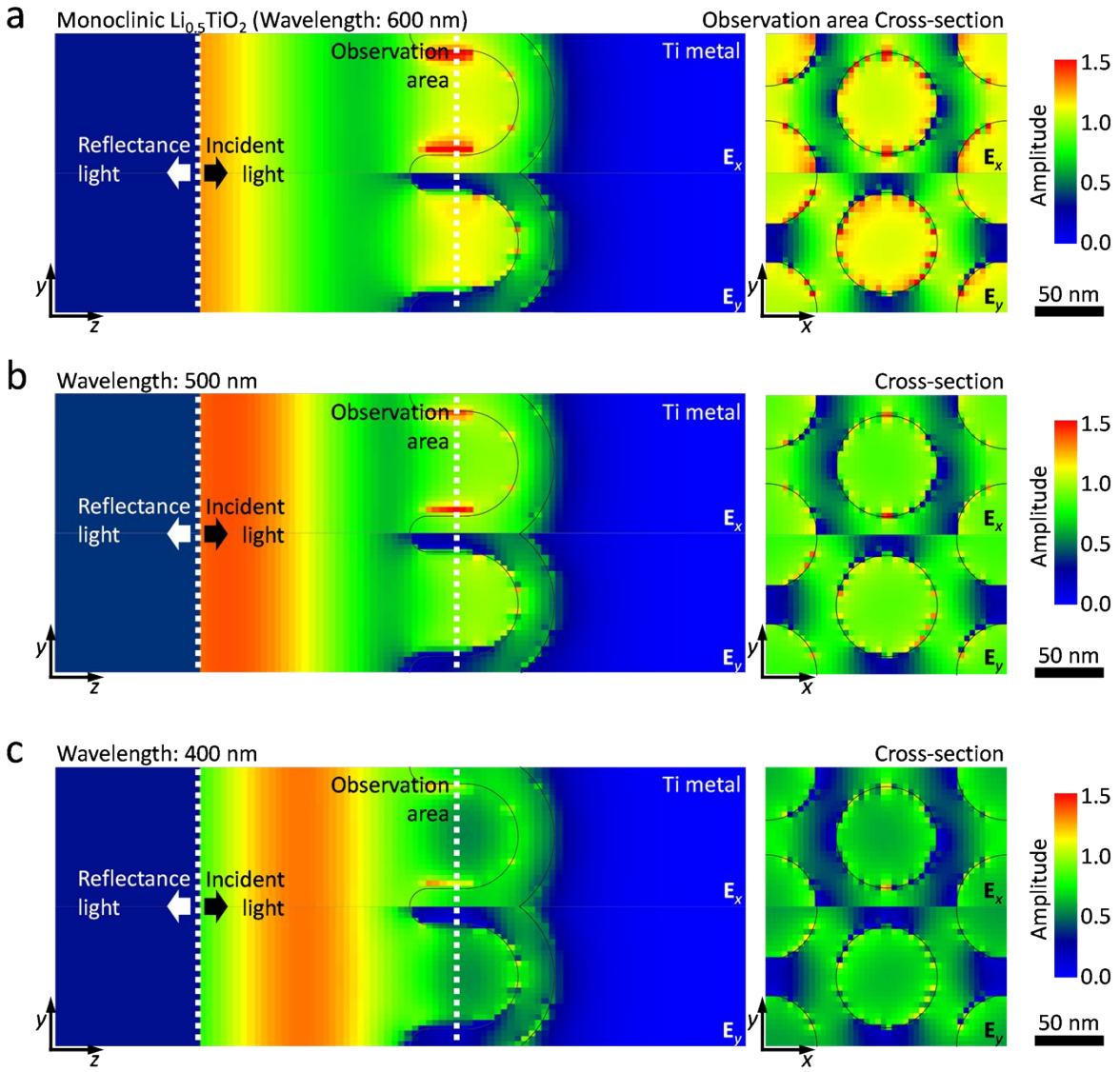

Supplementary Fig. S7. Simulated distribution of electric fields by the surface of monoclinic $Li_{0.5}TiO_2$ in the hexagonal nanostructure. Representative electric fields are shown at (a) 600, (b) 500 and (c) 400 nm wavelength, respectively.

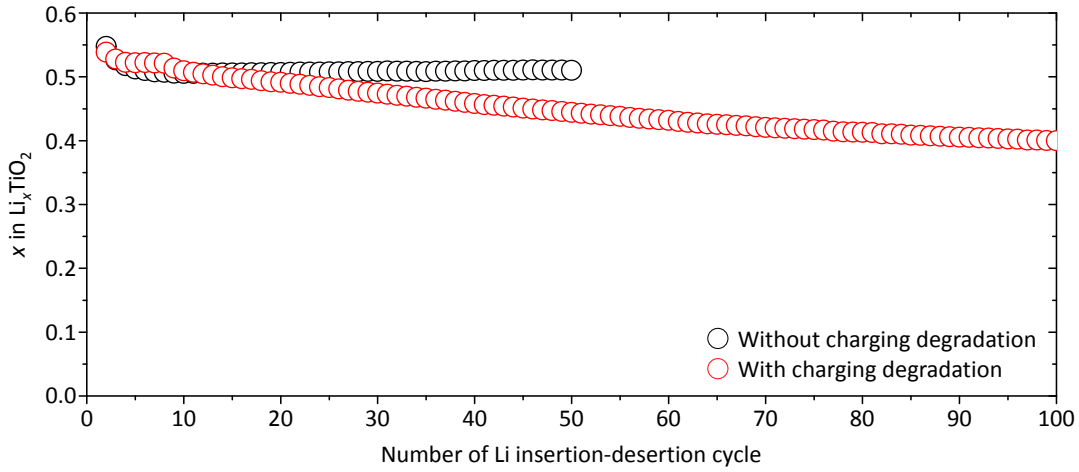

Supplementray Fig. S8. Occasional charging degradation of mixed-phase TiO_2 polymorph upon lithium insertion-deinsertion cycles. Although TiO_2 is usually stable from reversible lithium insertion (black circles), charging degradation intermittently occurs by un-known reasons (red circles).

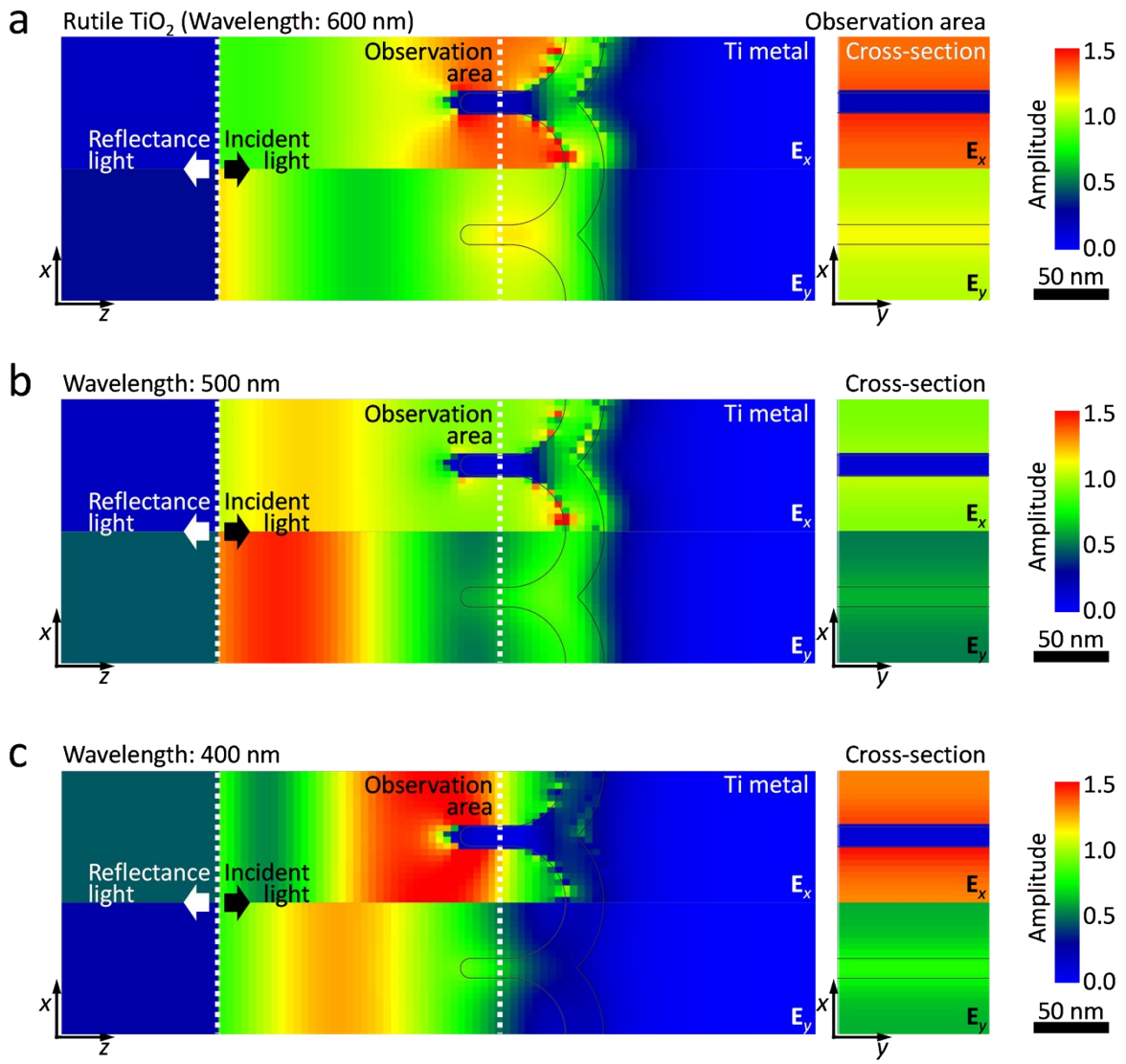

Supplementray Fig. S9. Simulated distribution of electric fields formed by the interference from the rutile TiO_2 film after the structural collapse. In comparison with the results shown in Fig. S5, formulations of E_x and Ey are significantly different from each other. Representative electric fields are shown at (a) 600, (b) 500 and (c) 400 nm wavelength, respectively.

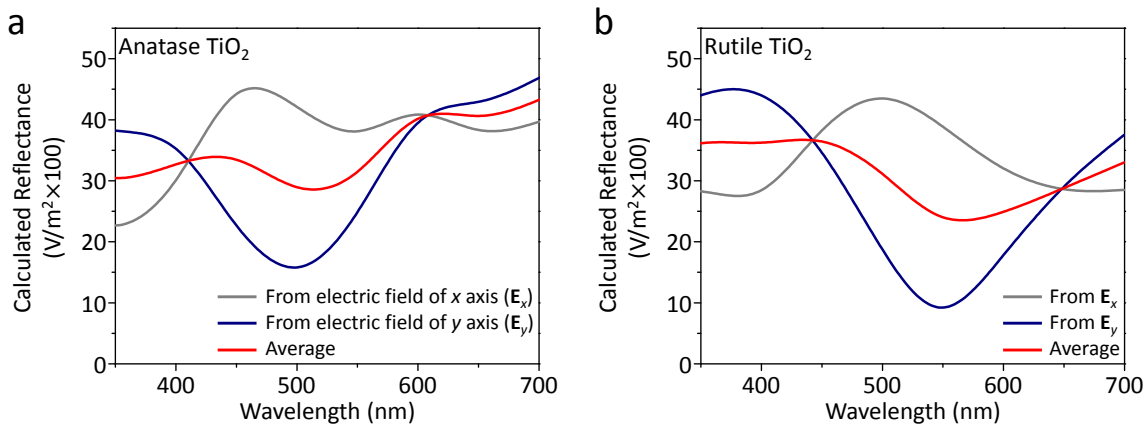

Supplementray Fig. S10 . Calculated reflectance spectra of anatase and rutile TiO_2 in collapsed structure. (a) Calculated reflectances of anatase TiO_2 were obtained from E_x (gray) and E_y (blue), respectively. The average is shown by the red line in Fig. 4d. (b) The identical calculating procedure was applied for rutile TiO_2. The average spectra from E_x and E_y are also exhibited in Fig. 4(d).